ELSEVIER

Ceramics International 32 (2006) 943–946

CERAMICS INTERNATIONAL

www.elsevier.com/locate/ceramint

Short communication

SnO_2 microparticles by thermal evaporation and their properties

Hyoun Woo Kim *, Seung Hyun Shim, Chongmu Lee

School of Materials Science and Engineering, Inha University, 253 Yong-Hyun-Dong, Nam-Ku, Incheon 402-751, South Korea

Received 4 April 2005; received in revised form 31 May 2005; accepted 21 June 2005
Available online 12 September 2005

Abstract

Agglomerated tin oxide (SnO_2) microparticles were fabricated by thermal evaporation of solid Sn powders. Samples were characterized by scanning electron microscopy, X-ray powder diffraction, transmission electron microscopy, and photoluminescence (PL) spectroscopy. As-prepared particles had diameters ranging from 0.2 to 1.3 μm, and appeared to be crystalline with tetragonal rutile SnO_2 structure. PL spectrum showed light emission in the visible field.

Keywords: SnO_2; Particles; Thermal evaporation

1. Introduction

Tin oxide (SnO_2) is a key functional material, which has multifaceted technological applications including optoelectronic devices [1,2] and gas sensors [3–6]. A variety of methods, such as sol–gel [7], pulsed laser deposition [8], wet-chemical synthesis [9–13], and thermal evaporation [14–16], have been used to produce SnO_2 nanoparticles with diameters below 100 nm.

In the present paper, we synthesized SnO_2 particles with diameters of more than several hundreds nanometers by a simple evaporation of Sn powders and investigated their structural and photoluminescence (PL) characteristics.

2. Experimental

Pure Sn powders were placed in an alumina boat, which was put in the middle of a quartz tube inserted in a horizontal tube furnace. We used thermally grown SiO_2 on Si(0 0 1) as a starting material onto which a layer of iridium (Ir) (about 150 nm) was deposited. On top of the boat, a piece of the substrate was placed with the Ir-coated side downwards. The vertical distance between the alumina boat and the substrate was approximately 10 mm. During the experiment, the furnace was kept at 850 °C for 2 h and a constant pressure with an air flow of 150 mTorr. Our previous experiments indicated that the mean diameter of synthesized particles increased with increasing the growth temperature in the range of 780–850 °C. After evaporation, the substrate was cooled down and then removed from the furnace for analysis. A white layer was found on the surface of the substrate.

Low angle (0.5°) X-ray diffraction (XRD: Cu $K\alpha_1$ radiation) patterns were obtained on a Philips X'pert MRD diffractometer with an incidence angle of 0.5°. Scanning electron microscopy (SEM) studies were carried out on a Hitachi S-4200. Further structural analysis using transmission electron microscopy (TEM) was performed on a Philips CM-200. For TEM observation, the products were ultrasonically dispersed in acetone, and then a drop of the suspension was placed on amorphous carbon films supported by copper grids and dried in air. PL spectrum was measured at room temperature by a 325 nm He–Cd laser (Kimon, 1K, Japan).

3. Results and discussion

Fig. 1 shows the XRD pattern of the powder which can be readily indexed to the tetragonal rutile structure of SnO_2 with lattice constants of $a = 4.738$ and $c = 3.187$ Å (JCPDS

* Corresponding author. Tel.: +82 32 860 7544; fax: +81 32 862 5546.
E-mail address: hwkim@inha.ac.kr (H.W. Kim).

0272-8842/$30.00
doi:10.1016/j.ceramint.2005.06.015

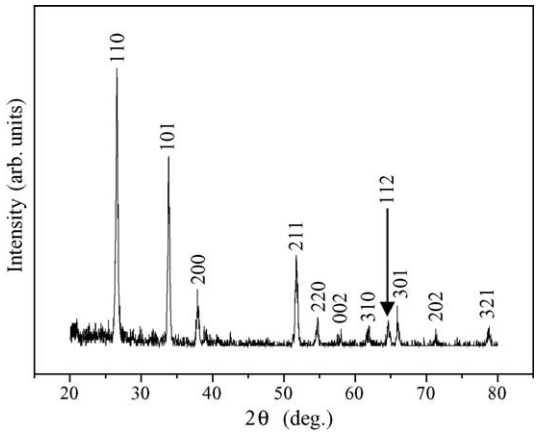

Fig. 1. XRD pattern of the products.

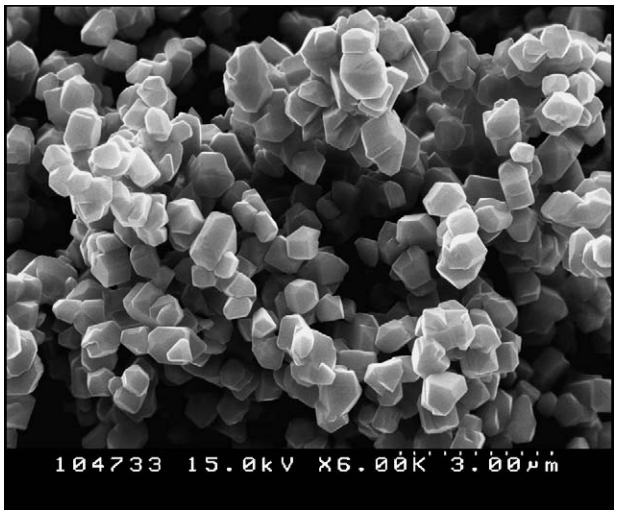

Fig. 2. SEM image of the products.

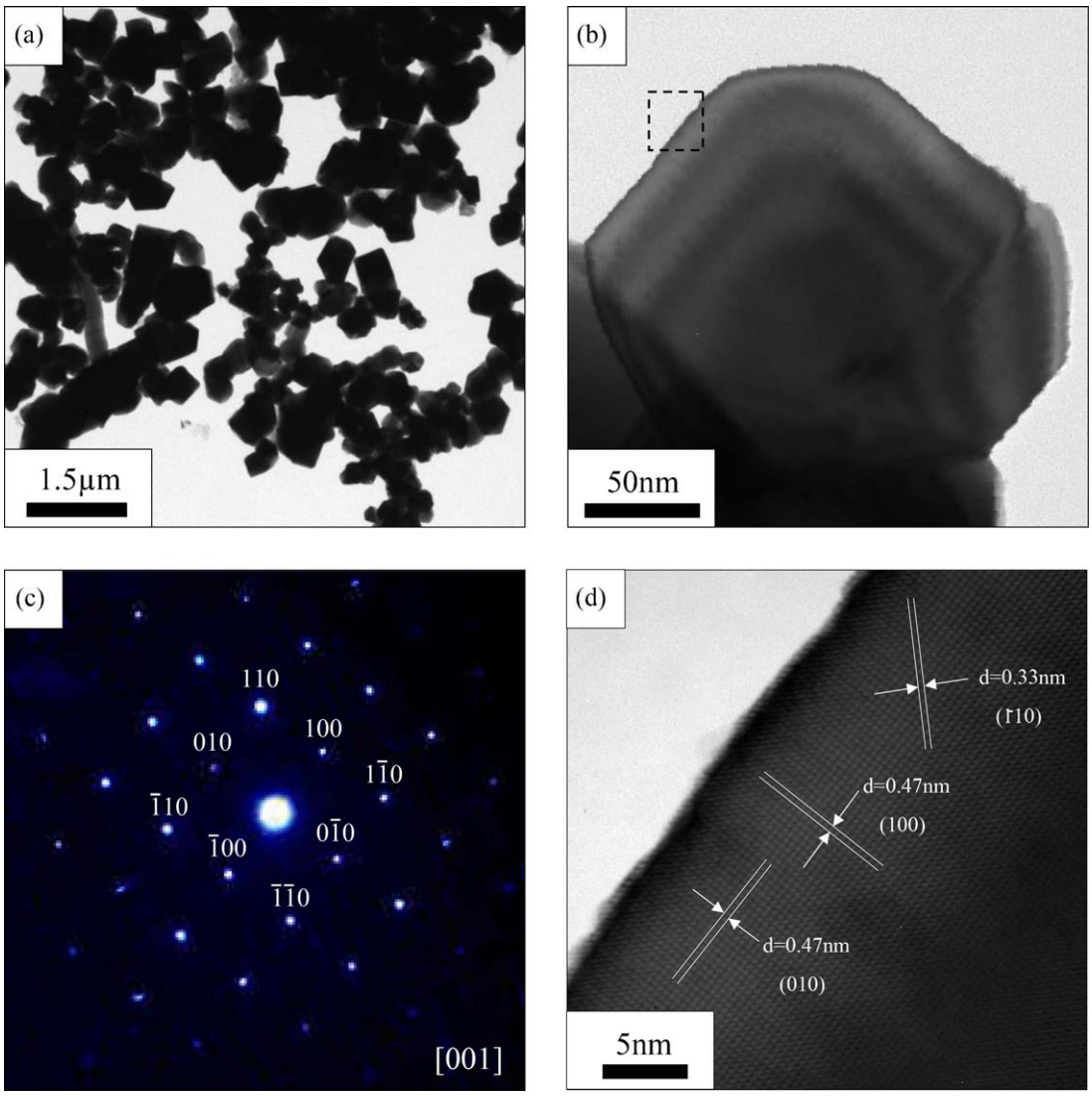

Fig. 3. (a) Low magnification TEM image of the products. (b) High magnification TEM image of a particle. (c) Corresponding SAED pattern. (d) HRTEM image corresponding to an area enclosed by the square in (b).

file no. 41-1445). No obvious reflection peaks from impurities, such as unreacted Sn or other tin oxides, were detected, indicating the high purity of the product.

The SEM image of Fig. 2 shows that the particles were obtained in an agglomerated state. Statistical analysis of many SEM images indicates that the SnO_2 particles have diameters ranging from 200 to 1300 nm and most particles are polyhedron-shaped with some facets.

A typical low magnification TEM image is shown in Fig. 3a. Fig. 3b gives a higher magnification TEM image of a single particle with a diameter of approximately 200 nm. The associated selected area electron diffraction (SAED) pattern (Fig. 3c) taken from the particle in Fig. 3b can be indexed as a tetragonal rutile SnO_2 single crystal, in good agreement with the XRD results presented above. Representative high resolution TEM (HRTEM) image of the particle, recorded near the side-edge of the SnO_2 particle shown in Fig. 3b, is given in Fig. 3d. Lattice fringes are clearly visible from the HRTEM image, revealing its single crystalline nature. The interplanar spacings are about 0.47, 0.47, and 0.33 nm, respectively, corresponding to the (0 1 0), (1 0 0), and (1 $\bar{1}$ 0) planes of rutile tetragonal SnO_2.

The air in the quartz tube is believed to provide the main source of oxygen for the growth of SnO_2 particles. The Sn atoms from Sn powder may react with O atoms to form metastable SnO, which subsequently decomposes into SnO_2 and Sn [17]. It is assumed that the precipitated solid SnO_2 on the Ir-coated substrates acts as a nucleus for the SnO_2 particles. Further work is in progress to assess the detailed synthesis mechanism.

PL spectrum carried out at room temperature is shown in Fig. 4. Visible emissions with a peak wavelength position of around 560–600 nm (corresponding to 2.07–2.22 eV) is dominantly observed. The visible light emission is known to be related to defect levels within the band gap of SnO_2, associated with O vacancies or Sn interstitials that have formed during the synthesis process [18–20]. Several researchers have previously reported similar emissions from SnO_2 nanoribbons [18] and SnO_2 nanorods [19].

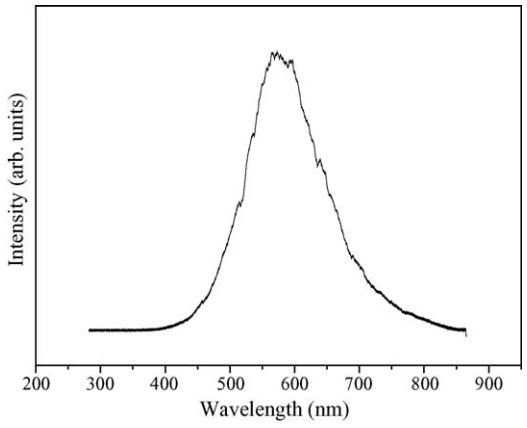

Fig. 4. Room temperature PL spectrum of the products with an excitation wavelength at 325 nm.

4. Conclusions

We have prepared SnO_2 particles by thermal evaporation of Sn powders in air flow. Structural and morphological characterization indicates that the polyhedral SnO_2 particles with the rutile structure have diameters ranging from 200 to 1300 nm. Optical measurements show that the SnO_2 particles generate a visible light emission that may be exploited in gas sensors or other optoelectronic devices.

Acknowledgement

This work was supported by Inha University Research Grant.

References

[1] A. Aoki, H. Sasakura, Tin oxide thin film transistors, Jpn. J. Appl. Phys. 9 (1970) 582.
[2] C. Tatsuyama, S. Ichimura, Electrical and optical properties of GaSe-SnO_2 heterojunctions, Jpn. J. Appl. Phys. 15 (1976) 843–847.
[3] E.R. Leite, I.T. Weber, E. Longo, J.A. Varela, A new method to control particle size and particle size distribution of SnO_2 nanoparticles for gas sensor applications, Adv. Mater. 12 (2000) 965–968.
[4] R.C. Aiyer, S.G. Ansari, P. Boroojerdian, R.N. Karekar, S.K. Kulkarni, S.R. Sainkar, Grain size effect on H_2 gas sensitivity of thick film resistor using SnO_2 nanoparticles, Thin Solid Films 295 (1997) 271–276.
[5] C. Nayral, E. Viala, V. Colliere, P. Fau, F. Senocq, A. Maisonnat, B. Chaudret, Synthesis and use of a novel SnO_2 nanomaterial for gas sensing, Appl. Surf. Sci. 164 (2000) 219–226.
[6] W.-P. Tai, J.-H. Oh, Preparation and humidity sensing behaviors of nanocrystalline SnO_2/TiO_2 bilayed films, Thin Solid Films 422 (2002) 220–224.
[7] F. Gu, S.F. Wang, M.K. Lü, G.J. Zhou, D. Xu, D.R. Yuan, Photoluminescence properties of SnO_2 nanoparticles synthesized by sol–gel method, J. Phys. Chem. B 108 (2004) 8119–8123.
[8] Z.W. Chen, J.K.L. Lai, C. H. Shek, H.D. Chen, Nucleation and growth of SnO_2 nanocrystallites prepared by pulsed laser deposition, Appl. Phys. A, published online.
[9] J.J. Zhu, Z.H. Lu, S.T. Aruna, D. Aurbach, A. Gedanken, Sonochemical synthesis of SnO_2 nanoparticles and their preliminary study as Li insertion electrodes, Chem. Mater. 12 (2000) 2557–2566.
[10] M. Ocana, C.J. Serna, E. Matijevi, Preparation and characterization of uniform nanocrystalline prismatic SnO_2 particles, Mater. Lett. 12 (1991) 32–36.
[11] Y. He, Y. Li, J. Yu, Y. Qian, Chemical control synthesis of nanocrystalline SnO_2 by hydrothermal reaction, Mater. Lett. 40 (1999) 23–26.
[12] H.-J. Ahn, H.-C. Choi, K.-W. Park, S.-B. Kim, Y.-E. Sung, Investigation of the structural and electrochemical properties of size-controlled SnO_2 nanoparticles, J. Phys. Chem. B 108 (2004) 9815–9820.
[13] T. Nütz, M. Haase, Wet-chemical synthesis of doped nanoparticles: optical properties of oxygen-deficient and antimony-doped colloidal SnO_2, J. Phys. Chem. B 104 (2000) 8430–8437.
[14] K.-M. Lee, D.-J. Lee, H. Ahn, XRD and TEM studies on tin oxide (II) nanoparticles prepared by inert gas condensation, Mater. Lett. 58 (2004) 3122–3125.
[15] V.M. Jimenez, A.R. Gonzalez-Elipe, J.P. Espinos, A. Justo, A. Fernandez, Synthesis of SnO and SnO_2 nanocrystalline powders

by the gas phase condensation method, Sens. Actuators B 31 (1996) 29–32.
[16] V.M. Jimenez, A. Caballero, A. Fernandez, J.P. Espinos, M. Ocana, A.R. Gonzalez-Elipe, Structural characterization of partially amorphous SnO_2 nanoparticles by factor analysis of XAS and ET-IR spectra, Solid State Ionics 116 (1999) 117–127.
[17] J.Q. Hu, X.L. Ma, N.G. Shang, Z.Y. Xie, N.B. Wong, C.S. Lee, S.T. Lee, Large-scale rapid oxidation synthesis of SnO_2 nanoribbons, J. Phys. Chem. B 106 (2002) 3823–3826.
[18] J. Hu, Y. Bando, Q. Liu, D. Goldberg, Laser-ablation growth and optical properties of wide and long single-crystal SnO_2 ribbons, Adv. Func. Mater. 13 (2003) 493–496.
[19] B. Cheng, J.M. Russell, W. Shi, L. Zhang, E.T. Samulski, Large-scale, solution-phase growth of single-crystalline SnO_2 nanorods, J. Am. Chem. Soc. 126 (2004) 5873–5972.
[20] S.-S. Chang, D.K. Park, Novel Sn powder preparation by spark processing and luminescence properties, Mater. Sci. Eng. B 95 (2002) 55–60.